



City Research Online

City, University of London Institutional Repository

Citation: Silvers, L. J. (2008). Long-term Nonlinear Behaviour of the Magnetorotational Instability in a Localised Model of an Accretion Disc. *Monthly Notices of the Royal Astronomical Society*, 385(2), pp. 1036-1044. doi: 10.1111/j.1365-2966.2008.12906.x

This is the unspecified version of the paper.

This version of the publication may differ from the final published version.

Permanent repository link: <https://openaccess.city.ac.uk/id/eprint/1353/>

Link to published version: <https://doi.org/10.1111/j.1365-2966.2008.12906.x>

Copyright: City Research Online aims to make research outputs of City, University of London available to a wider audience. Copyright and Moral Rights remain with the author(s) and/or copyright holders. URLs from City Research Online may be freely distributed and linked to.

Reuse: Copies of full items can be used for personal research or study, educational, or not-for-profit purposes without prior permission or charge. Provided that the authors, title and full bibliographic details are credited, a hyperlink and/or URL is given for the original metadata page and the content is not changed in any way.

City Research Online:

<http://openaccess.city.ac.uk/>

publications@city.ac.uk

Long-term Nonlinear Behaviour of the Magnetorotational Instability in a Localised Model of an Accretion Disc

L. J. Silvers*

Laboratoire de Radioastronomie, Departement de Physique Ecole Normale Supérieure, 24 Rue Lhmond, 75231, Paris, 05, France.

ABSTRACT

For more than a decade, the so-called shearing box model has been used to study the fundamental local dynamics of accretion discs. This approach has proved to be very useful because it allows high resolution and long term studies to be carried out, studies that would not be possible for a global disc.

Localised disc studies have largely focused on examining the rate of enhanced transport of angular momentum, essentially a sum of the Reynolds and Maxwell stresses. The dominant radial-azimuthal component of this stress tensor is, in the classic Shakura-Sunayev model, expressed as a constant α times the pressure. Previous studies have estimated α based on a modest number of orbital times. Here we use much longer baselines, and perform a cumulative average for α . Great care must be exercised when trying to extract numerical α values from simulations: dissipation scales, computational box aspect ratio, and even numerical algorithms all affect the result. This study suggests that estimating α becomes more, not less, difficult as computational power increases.

Key words: accretion discs; magnetic fields; instabilities

1 INTRODUCTION

Linear stability analysis has shown that a differentially rotating disc, with angular velocity decreasing outwards, is unstable in the presence of a weak magnetic field (see, for example, Balbus & Hawley (1991); Balbus & Hawley (1992)). This magnetorotational instability (MRI) gives rise to turbulence within the disc and is a plausible way that efficient outward transport of momentum in a disc can be realised (Balbus & Hawley (1998)). However, while this is an appealing concept, it is crucially important, due to the non-linear form of the governing equations, to investigate the non-linear evolution and saturation of this instability to determine if this is indeed a route by which angular momentum transport can be achieved on the required time-scales.

The equations that govern the evolution within a disc are computationally demanding to evolve. Therefore, in order to study the evolution and saturation of key quantities associated with this instability (e.g. stresses, energies etc), it is useful to employ a localised, ‘shearing-box’ model (see, for example, Brandenburg, Nordlund, Stein & Torkelsson (1995); Hawley, Gammie & Balbus (1995)). This approach has proved useful as it has enabled higher local resolutions to be achieved for the same computational cost as that for a full

disc simulation. However, while a localised approach does facilitate longer runs and higher resolutions, at the point of the early shearing box calculations the resources were such that only modest run times (usually less than 30 orbits) were possible (see, for example Hawley, Gammie & Balbus (1995)).

When discussing the MRI, the principal quantity of interest is α , which is related to the rate of angular momentum transport in a disc. This quantity is defined as (Shakura & Sunyaev (1973); Hawley, Gammie & Balbus (1995)):

$$\alpha = w_{xy}/P \tag{1}$$

In this definition, P is the gas pressure and w_{xy} is a component of the $x - y$ stress tensor i.e.

$$w_{xy} = \rho v_x v_y - \frac{B_x B_y}{4\pi}, \tag{2}$$

where ρ denotes density; v_x is the x component of the velocity field; v_y is the perturbed component of the velocity field in the y direction; B_x is the x component of the magnetic field and B_y is the y component of the magnetic field.¹

In turbulent flows transport quantities such as α are

¹ Note here that (x,y) refers to a local set of coordinates in (r, ϕ) and not $(-\phi,r)$ as sometimes utilised in certain hydrodynamical models.

* E-mail: lara.silvers@lra.ens.fr (LJS)

highly fluctuating. The resource constraints at the time of the earliest calculations forced α values to be quotes from by a simple average over a modest number of orbits, which is useful to give an idea of the order of magnitude of this quantity (see, for example, Hawley, Gammie & Balbus (1996)). However, unless an extremely large number of orbits is considered, the saturation level will vary as you increase the number of orbits over which the average is evaluated. This can, make it difficult to see clearly the effect if varying each of the parameters (e.g. dissipation scale, domain size etc) associated with the problem. It is better, if the resources are available, to calculate a cumulative average for this fluctuating quantity. This does require vast numbers of computer hours, which is only recently possible. As such, the principal aim of this paper is to calculate long-time cumulative averages of α .

In order to keep the computational costs acceptable, we choose to make several simplifying assumptions in this paper. First, we choose to initially work in a cubic domain, which is only relaxed later in the paper. This enabled us to explore the effect of decreasing the dissipation scale on the cumulative average α and to show that small scales are playing a role in determining the saturation level of this quantity. The second simplification is that we chose to solve the ideal MHD equations. This reduces the cost of the calculation by a significant fraction though it does mean that all calculations are at an effective Prandtl number of order unity. This is acceptable as in this particular investigation we were not trying to examine the effect of varying the Prandtl number. Indeed, this has recently been considered (Lesur & Logaretto (2007); Fromang, Papaloizou, Lesur, Heinemann (2008)). The work in this paper is aimed, somewhat, to complement these recent works even though here we do not explicitly include dissipation coefficients. We will show that, as in the Lesur & Logaretto (2007) paper the effect of increasing resolution for a fixed box size is to increase α . Further, we show that the effect of increasing the box length is to decrease the saturation level of α as the parasitic instability is allowed to take hold.

The paper will proceed as follows: In section 2 we will fully detail our model and the numerical method used in the solution of the governing equations. We will discuss the results in section 3. This section is divided into two subsections. In section 3.1 we begin by showing the problems that are encountered in standard shearing box calculations that makes long-term cumulative averages difficult to calculate. We show that this problem is a result of compounded errors that come from the shearing boundary conditions. We then present a correction to the numerical algorithm, which permits us to calculate long-term cumulative averages and show how α varies with resolution (or dissipation length scale). In section 3.2 we bring the results section to a close by showing that the effect of increasing the length of the box in the azimuthal direction is to decrease α . In Section 5 we summarise the finding as well as discuss the astrophysical consequences.

2 THE MODEL

In this paper we restrict consideration to a local patch of a Keplerian disc and to use the shearing box approximation. Within this paper we choose to follow the strategy of many of the earlier works by which we mean that we will consider an ideal MHD problem. We shall assume for simplicity in this paper that the z -component of gravity is suitably small and so may be neglected (assumed to be within a pressure scale height of the midplane of the disc). Further we assume that the gas is isothermal. As such, equation set may be written as:

$$\frac{\partial \rho}{\partial t} + \nabla \cdot \rho \mathbf{v} = 0 \quad (3)$$

$$\begin{aligned} \frac{\partial \mathbf{v}}{\partial t} + \mathbf{v} \cdot \nabla \mathbf{v} = & - \frac{1}{\rho} \nabla \left(P + \frac{B^2}{8\pi} \right) + \frac{\mathbf{B} \cdot \nabla \mathbf{B}}{4\pi\rho} - 2\boldsymbol{\Omega} \times \mathbf{v} \\ & + 2q\boldsymbol{\Omega}^2 x \hat{\mathbf{x}} \end{aligned} \quad (4)$$

$$\frac{\partial \mathbf{B}}{\partial t} = \nabla \times (\mathbf{v} \times \mathbf{B}) \quad (5)$$

$$\nabla \cdot \mathbf{B} = 0 \quad (6)$$

$$P = c_s^2 \rho \quad (7)$$

where we obey the standard notational convection and thus, ρ denotes density, P denotes the gas pressure, v and B are the velocity and magnetic fields, respectively, Ω is the angular velocity, $q = -d \ln \Omega / d \ln R$.

Our work will differ from earlier works in the following ways. First we choose to start from a perturbation that has a specific analytic form that is not a random perturbation at each of the grid points. This initial perturbation in such simulations are immaterial so long as they are small in amplitude. However, in order to be completely clear on our starting condition, we choose to start from a perturbation that can be expressed in a simple analytic manner so that we have a consistent start condition as we vary the resolution. We choose to perturb each of the velocity components in the following manner:

Defining

$$f_x = \sum_{n=1}^5 \sin[2\pi n x - (1.2 - 0.2n)], \quad (8)$$

$$f_y = \sum_{n=1}^5 \sin[2\pi n y - (1 - 0.2n)], \quad (9)$$

$$f_z = \sum_{n=1}^5 \sin[2\pi n z - (0.8 - 0.2n)] \quad (10)$$

the initial velocity components are then expressible as:

$$v_x = 0.01\Omega f_x f_y f_z \quad (11)$$

$$v_y = -q\Omega x + 0.01\Omega f_x f_y f_z \quad (12)$$

$$v_z = 0.01\Omega f_x f_y f_z \quad (13)$$

We have chosen this particular form to give the perturbation

Table 1. Summary of all the cases presented in the paper

Case	Resolution	Aspect Ratio	Artificial Viscosity	Mean Cleaning
1	32 : 32 : 32	1:1:1	No	No
2	64 : 64 : 64	1:1:1	No	No
3	128 : 128 : 128	1:1:1	No	No
4	32 : 32 : 32	1:1:1	Yes	No
5	64 : 64 : 64	1:1:1	Yes	No
6	32 : 32 : 32	1:1:1	No	Yes
7	64 : 64 : 64	1:1:1	No	Yes
8	128 : 128 : 128	1:1:1	No	Yes
9	64 : 128 : 64	1:2:1	No	Yes
10	64 : 192 : 64	1:3:1	No	Yes
11	64 : 384 : 64	1:6:1	No	Yes

some complexity while still keeping it simple to code and express.

In this work we choose to start from a uniform density and so apply no perturbation to this quantity. We take $\rho_0 = 1$, $P_0 = 10^{-6}$, $\Omega = c_s = 10^{-3}$ and q is taken to be that for a Keplerian profile namely, $3/2$. The embedded magnetic field is uniform, in the vertical-direction and such that $\beta = 800$.

Initially, unlike in most of the earlier works we choose to consider a shearing box where each side is of unit length i.e. one that has the same length and number of grid points in each directions. Such an approach facilitates probing to higher resolutions without resorting to earlier methods of assuming *a priori* that less resolution is required in the y -direction. While less resolution might be warranted in the y -direction in simulations that have a clear difference in the scale of the structures in each of the spacial directions we choose here to use caution and not make this assumption which, amongst other things, gives rise to an anisotropy in the numerical dissipation.

The equations, given above, are solved with a parallel finite-difference time-explicit code. The code is essentially just a parallelized version of the serial ZEUS code that is freely available. As in earlier papers (e.g. Stone & Norman (1992); Hawley & Stone (1995); Hawley, Gammie & Balbus (1996)) we use the method of constrained transport scheme for magnetic advancement so that the $\nabla \cdot \mathbf{B} = 0$ is enforced to the accuracy of the machine. In this work we use the standard shearing-box boundary conditions. Thus the domain is periodic in both the y and z directions and shearing-periodic in x (see Hawley, Gammie & Balbus (1996) for further details). This code contains an adaptive step size that is multiplied, as is standard, by a safety factor. We have conducted several tests to ensure that the step size does not give rise to numerical instability. This check involved varying the safety factor in this code to ensure that all prominent global features, trends and saturation levels are fully captured by the integration, which could be referred to as a check that we have the ‘true’ or ‘converged’ solution.

3 RESULTS

Before beginning to discuss the finding it helpful to provide an overview of all cases at this point. Table 1 shows each of the cases that we have considered. We have used the method

detailed in Hawley, Gammie & Balbus (1995) to ensure that the fastest growing wavelength is resolved.

We will choose to split the results section into two halves. Firstly we will discuss the effect of increasing the resolution and then we will go on to discuss the effect of increasing the box length, in the y direction, while maintaining the same resolution per unit length.

3.1 Ideal MHD

We begin the discussion of the results with our fiducial model, case 1. In this model we consider a resolution of 32 grid points in each of the three directions. This fiducial model is at a similar resolution, in the x and y directions, as can be found in many of the original calculations. This said, the earlier calculations did typically a longer box length than we do here. This deliberate change was made for two reasons. First, the decrease in the box size enables us to push to much higher resolutions. Second, and most importantly for what we wish to examine here, an increased integration time i.e. such a reduction in the box length facilitates being able to ascertain many more orbits for the same computational cost. We shall discuss the ramifications of increasing the box length later in the paper and some comments on the effect of varying the computational domain can be found in Winters, Balbus & Hawley (2003).

As stated in the introduction, we wish to determine a cumulative average for the quantity α , which is related to the difference of the Reynolds and Maxwell stresses. Such a quantity can only be calculated if the simulations are run for sufficiently long so that there is a large time in the saturated state for the cumulative average to settle. Figure 1 shows the initial section evolution of the magnetic and kinetic energies for the 32^3 case and illustrates the it can take several orbits for the saturated state to begin. We note that, despite the reduction in the box size, these figures resemble those from the earlier calculations. However, we note that time to reach a statistically steady state occurs at a later point in terms of the number of orbits but at a comparable time from the start of the simulations. Other slight differences from earlier calculations are combined effect of box size, isothermality and choice of plasma β .

These figures appear to show that the evolution is complete and that the final state has been obtained and thus one might think that all that remains to calculate a cumulative average is to carry the calculation on for sufficient time and then evaluate the cumulative average of α . However, figure 2 shows that, in this calculation, what appears to initially be a statistically steady state is only approximately so. If you examine the solution for 1000 orbits one sees that the first 200 orbits or so is in fact a slow ramp up to a higher saturation level.

The most important implication from a shift in the average magnetic and kinetic energies is that this is almost certainly a corresponding shift in the momentum transport and figure 2 shows that this is indeed the case. However, from a figure of this kind it is exceptionally hard to gain a feeling for the structure —indeed much of the information on the temporal variability is being lost. As such, we provide a more detailed series of snapshots over the full 1000 orbits in 3. This images show that the system is moving from a state which is rather turbulent into a state where there is a

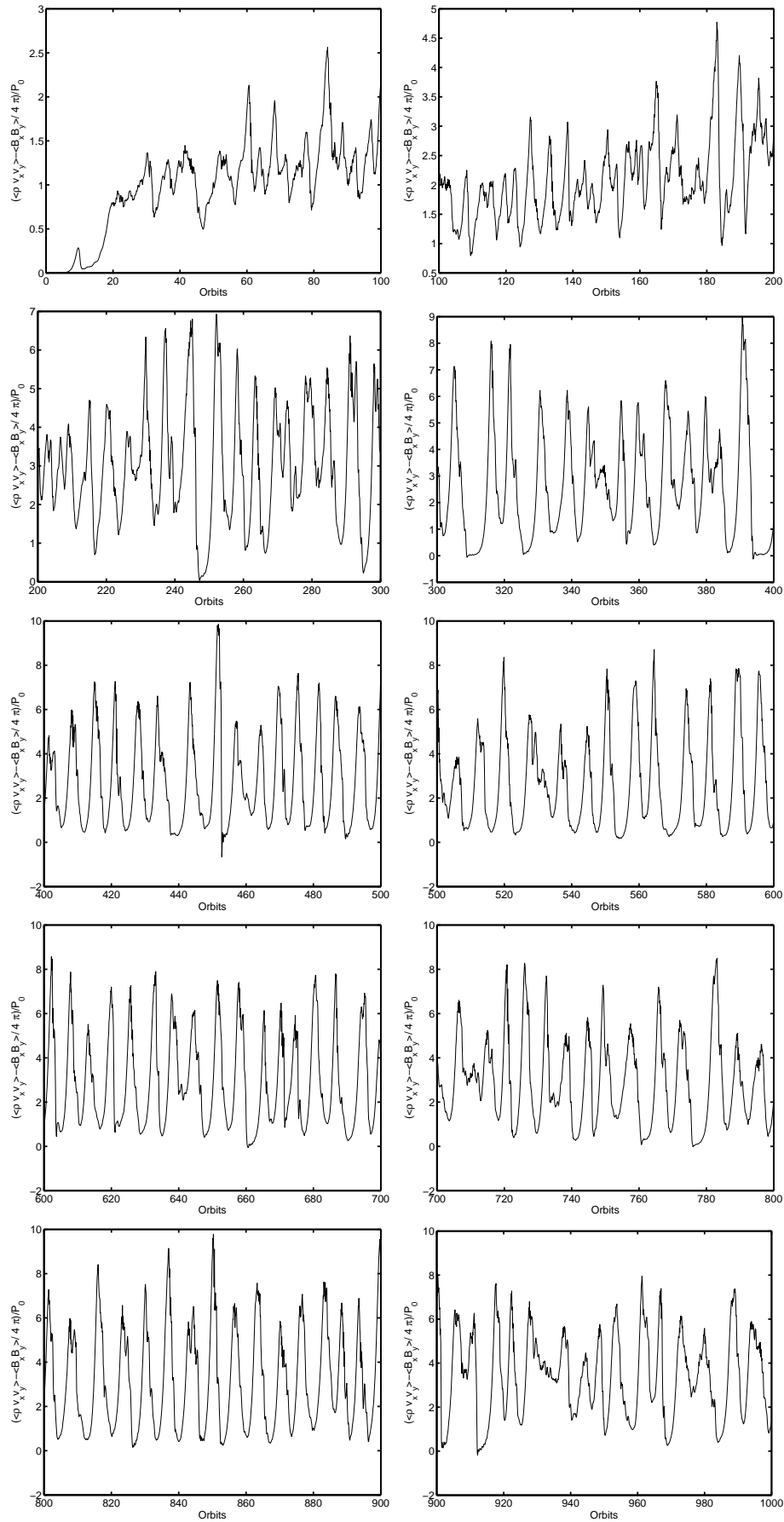


Figure 3. A series of plots showing in more detail the evolution of α as the number of Orbits increases for case 1

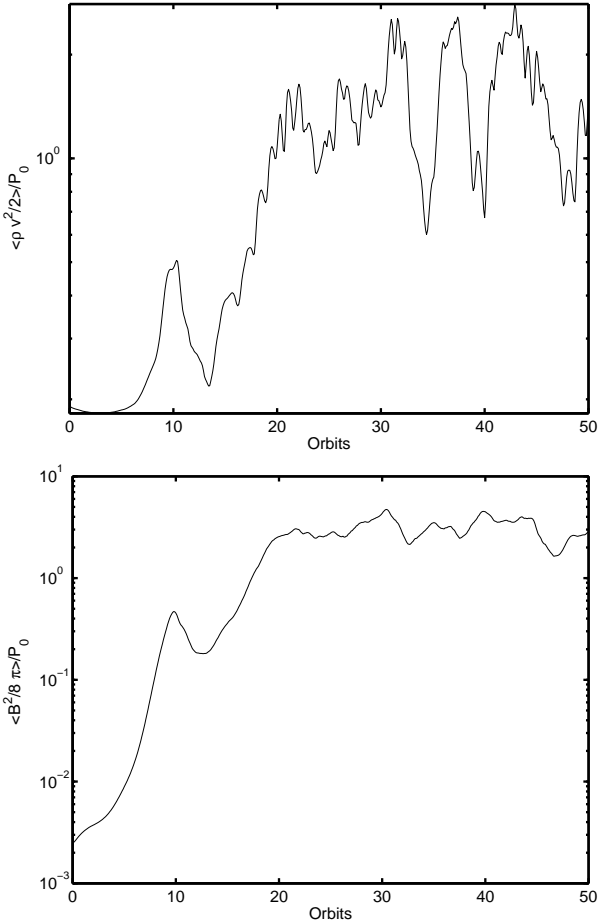


Figure 1. Top: Kinetic energy evolution for the fiducial case for the first 50 Orbits. Bottom: Magnetic energy evolution (normalised) for the fiducial case for the first 50 orbits.

repeated classical channel solution presenting before being destroyed and the cycle repeating.

In the light of the images show above, one of the most natural questions concerns whether the same behaviour is still found if the length-scale for the dissipation scale is decreased. In this problem this is akin to increasing the number of grid points that are used. As such we have examined the case when the number of grid points in each spatial direction and the findings are shown in figure 4. Note that, while the climb to the saturated state is slightly slower in this case, a transition from one quasi-statistically steady state to another still occurs. Similar was found at a resolution of 128^3 and so we conclude that this behaviour is independent of the length-scale for dissipation.

3.1.1 Artificial Viscosity

In the above calculations we have not included a resistivity or a viscosity of any kind and have just left the dissipation to be the result of the grid. However, there in several of the local shearing box calculations there was an artificial viscosity term included in the equation of motion of the form (Hawley, Gammie & Balbus (1996)):

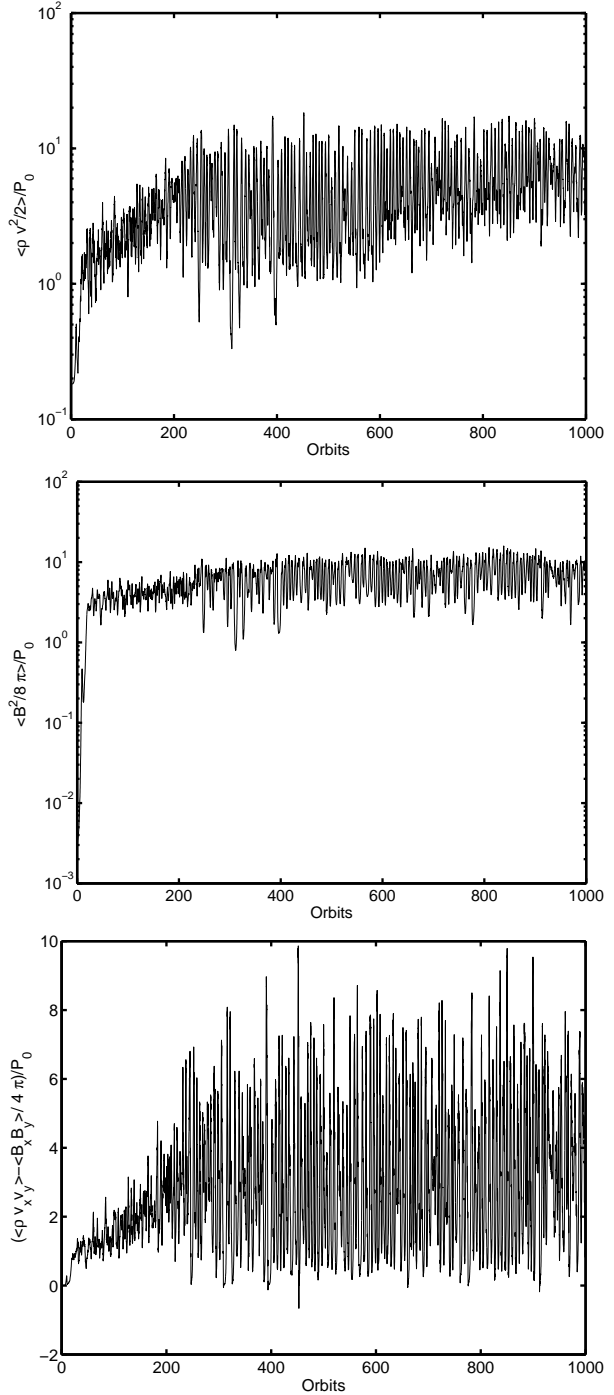


Figure 2. Top: Kinetic energy evolution (normalised) for the case 1 for 1000 orbits. Middle: Magnetic energy evolution (normalised) for case 1 for 1000 orbits. Bottom: The evolution of α for case 1.

$$A = C\rho(\delta_i v_i)(\Delta x) \tag{14}$$

The motivation for such a term was to provide limited extra dissipation in the case when there is a strong compressional solution. As such, it retains the original ideal magnetohydrodynamic (MHD) nature of the equations and only calls for extra assistance in special situations. While we

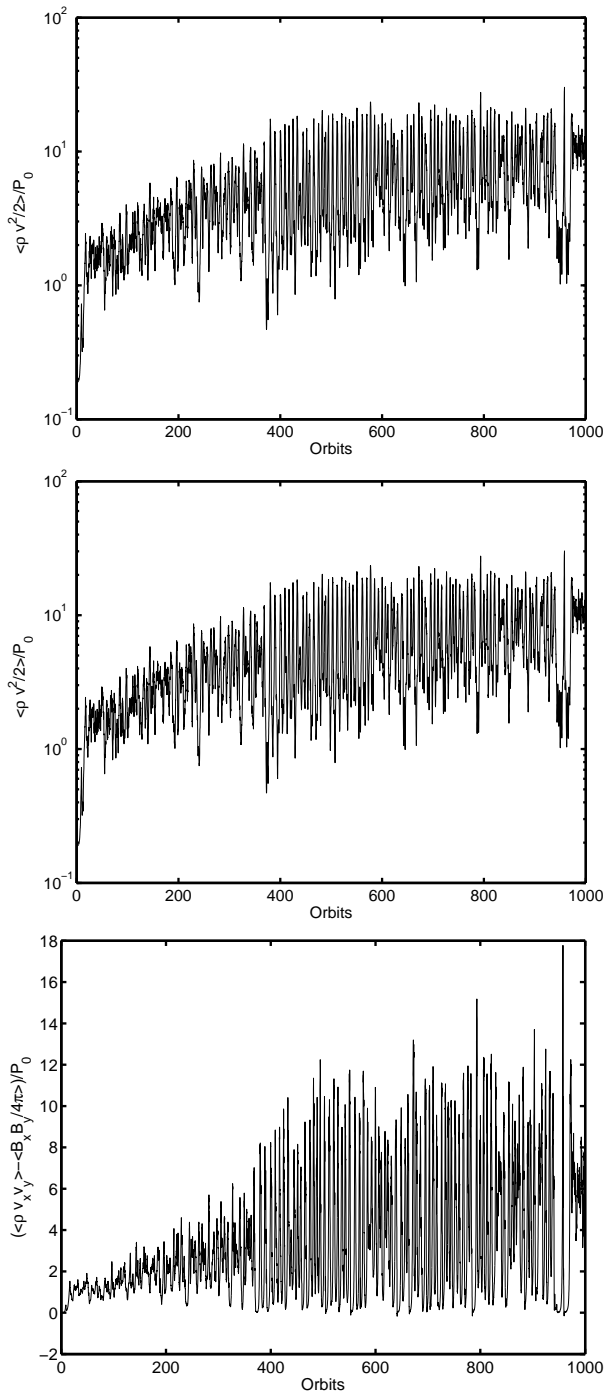


Figure 4. Top: Kinetic energy evolution (normalised) for case 2 for 1000 orbits. Middle: Magnetic energy evolution (normalised) for case 2 for 1000 orbits. Bottom: The evolution of α for the case where there are 64^3 grid points (case 2).

would argue that a viscosity of some kind is useful we would argue that it is much better to consider a physical viscosity that acts continually.

However, while we do not believe that the artificial viscosity method is the most instructive it is a method that has served the community for many years and, as such, one must entertain the possibility that the solutions found

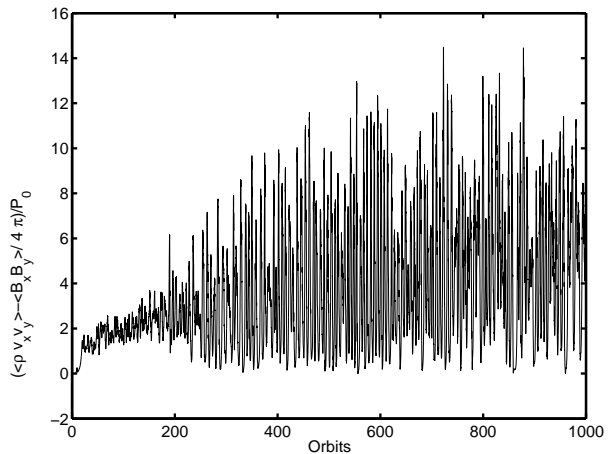


Figure 5. The evolution of α for the case where there are 32^3 grid points and an artificial viscosity (case 4).

about might in some way be the result of the lack of the inclusion of an artificial viscosity. As such, for completeness we here examine the 32^3 calculation with the artificial viscosity term included and where $C = 2.0$ as is standard. This implies that smoothing is carried out over two cells. Further discussion of the artificial viscosity can be found in Hawley, Gammie & Balbus (1996) and Stone & Norman (1992).

Figure 5 shows that the same global trend is witnessed in this case as in the case where there is no artificial viscosity included. This shows that the inclusion of an artificial viscosity does not change the result found above.

3.1.2 Problems with the Shearing Boundary Conditions

The behaviour witnessed above is fully explained by an examination of what occurs to the mean of the various components. Many of these components should formally be zero but the interpolation necessary in the implementation of the shearing boundary conditions give rise to errors as shown in figure 6. These errors have been mentioned before in earlier calculations Hawley, Gammie & Balbus (1995). However, many of the early calculations were for short time spans and there the error was stated to be about $10^{-3} c_s$. While we confirm that this is true for small numbers of orbits this is not true in the long term. In fact, as figure 6 shows the mean B_z and B_y fields both grow and that the B_y field grows to such an extent that it becomes of greater magnitude. We note here that the numerical method employed prevents B_x from obtaining significant error. The constrained transport forces B_x to stay constant to round off because it is evolved with the emf components E_y and E_z which are strictly periodic and hence B_x is conserved to round off error. However, both B_y and B_z have some error due to the shearing box interpolation in E_x .

If we are to obtain a valid long-term average for α then we need to remove this error, which compounds to give us an unintentional switch in the mean field. As such we proceed by forcing all mean values to their mathematically formal values by removing the error at set intervals. Obviously the most rigorous correction would be to invoke this cleaning procedure every time-step. However, this is computationally

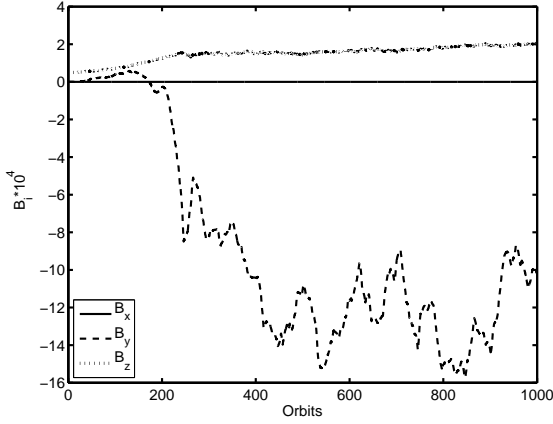


Figure 6. The evolution of each of the components of the magnetic field for case 1.

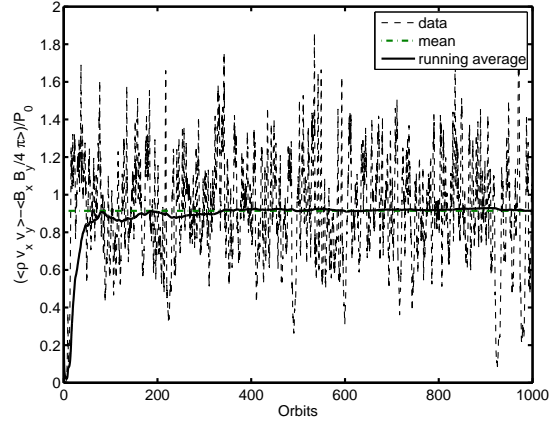


Figure 9. The evolution of α when full cleaning is employed for case 7 (1:1:1 aspect ratio)

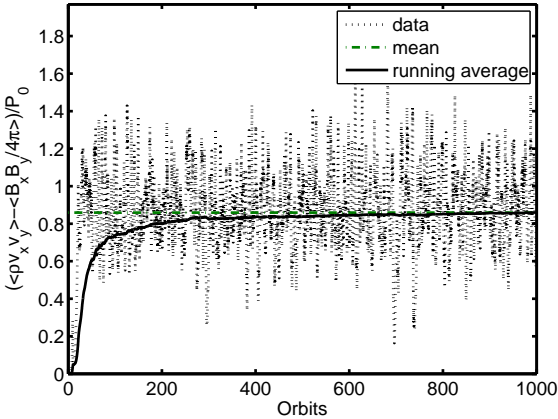


Figure 7. The evolution of α when full cleaning is employed for case 6 (1:1:1 aspect ratio)

demanding. Therefore, we choose here to correct the mean values every 100 time-steps as we determined that this gives phenomenally good agreement with cleaning every time-step for considerably less cost.

Figure 7 shows the new temporal evolution of α once the cleaning has been carried out for the 32^3 , which is case 6. It is clear that the effect of cleaning the mean values on α is to continue with the saturated level that we witnessed in the first part of figure 2. Therefore, it is now possible to evaluate the cumulative average until it saturates. Figure 7 not only shows the cumulative average but also the mean value for this case. Figure 8 shows a more detailed series of snapshots for α in this case and clearly shows that the randomised, turbulent, behaviour persists for all time and we do not now move to a repeated channel solution case.

The primary aim of this paper was to examine the effect of decreasing the dissipation scale (by increasing the resolution) and we are now in a position to do so. Figure 9 show the effect of doubling the resolution (decreasing the dissipation scale) on α . We note that the average value is increased as resolution is increased. This fact is amplified by the data

Table 2. Selected cases together and the associated α from a cumulative average

Case	Resolution	Box dimension	α
6	32:32:32	1:1:1	0.85
7	64:64:64	1:1:1	0.94
8	128:128:128	1:1:1	1.02
9	64:128:64	1:2:1	0.43
10	64:192:64	1:3:1	0.29
11	64:384:64	1:6:1	0.16

in table 2 (cases 6-8), which shows a clear upward trend as resolution is increased. As such, this shows that small scales are important in these calculations and the level at which the dissipation scale is set is crucial in determining that rate of enhanced transport.

3.2 The Effect of Increasing the Box length

In the above section we chose to focus on a domain where the aspect ratio is 1 : 1 : 1. This was selected to facilitate the longer time calculations at higher resolutions. However, as the earlier calculations considered a 1 : 2π : 1 and so in this section we examine what happens at modest resolutions to the saturated level of α . We have considered boxes with the aspect ratios 1 : 2 : 1, 1 : 3 : 1 and 1 : 6 : 1. The effect of elongating the is summarised in 2 (cases 7, 9-11) and the evolution is shown in figure 10.

There is a clear decrease in the saturation level as the box is increased in the azimuthal direction. What we are seeing is the effect that in short box lengths the parasitic instability is limited (see Goodman & Xu (1994) for more details on this instability).

4 CONCLUSIONS

In this paper we have returned to the original concept to understand turbulent transport of angular momentum in an accretion disc. As such, we considered the standard local

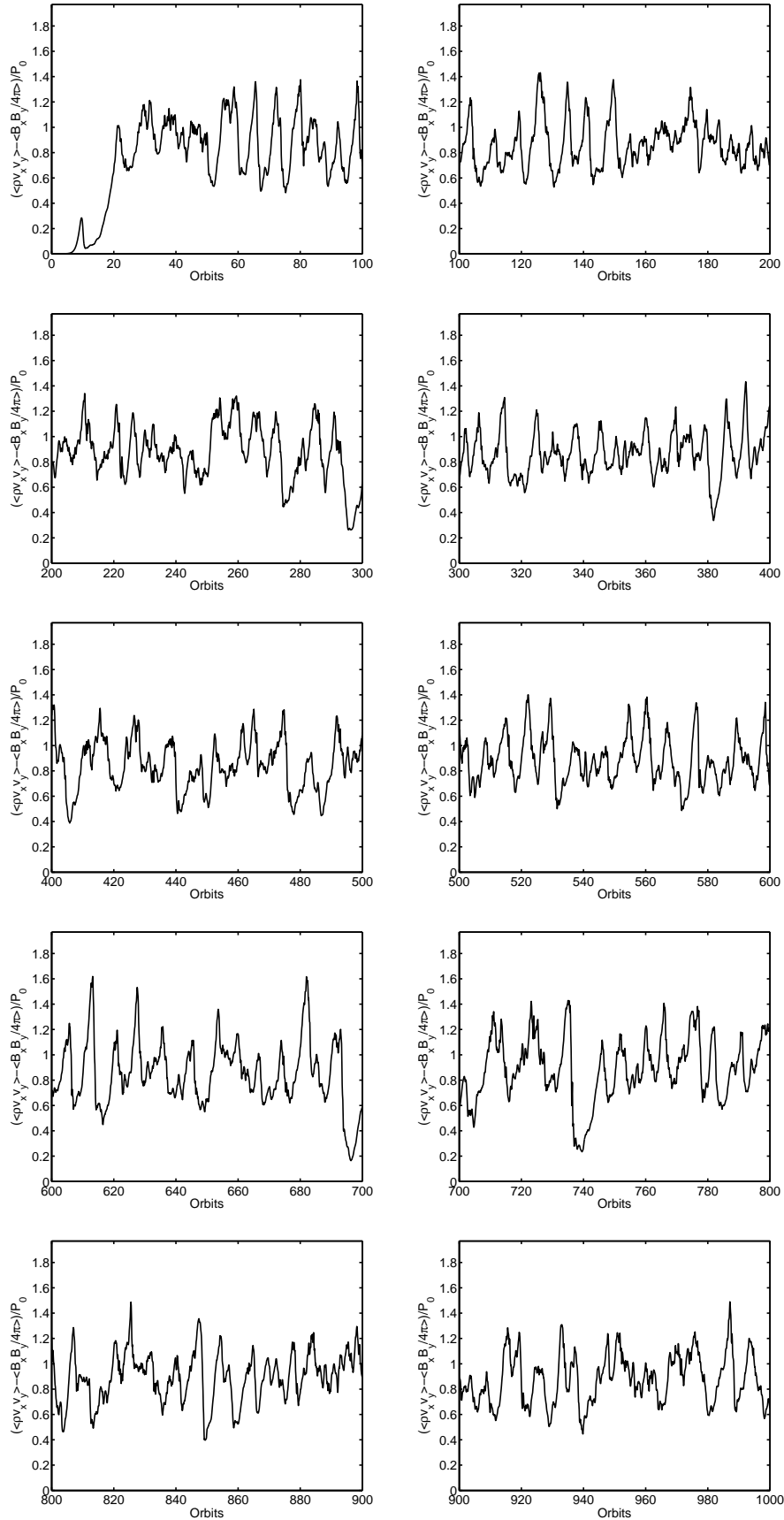


Figure 8. A series of figures showing the time evolution of α when 'cleaning' is employed for case 6.

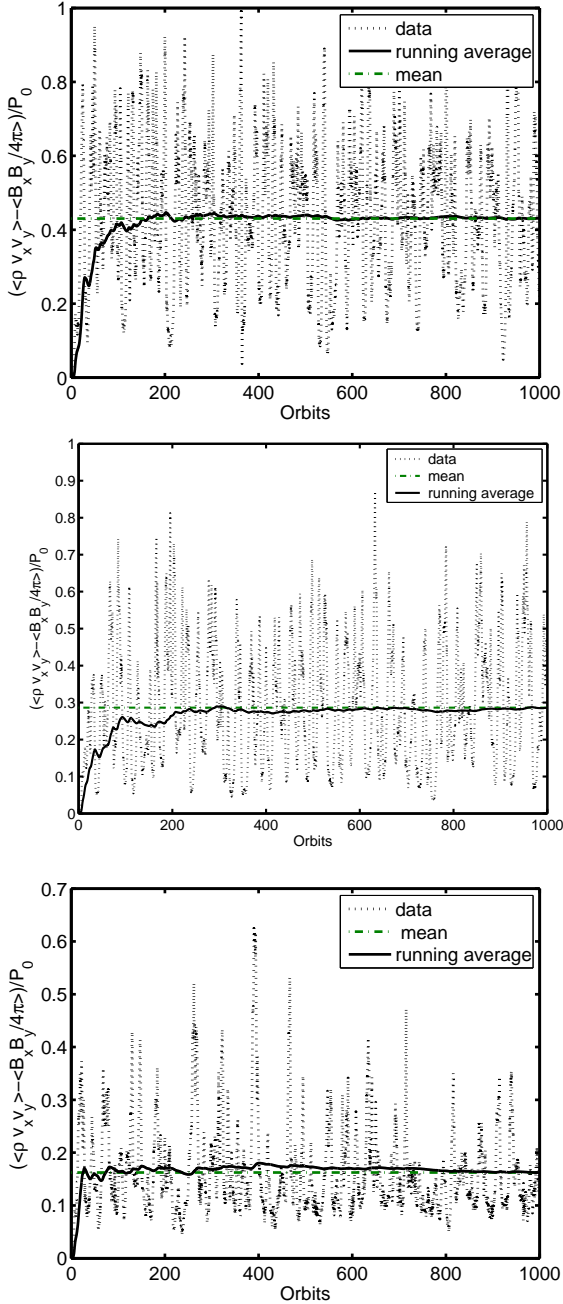


Figure 10. Top: The evolution of α when full cleaning is employed for case 9 (1:2:1 aspect ratio). Middle: The evolution of α when full cleaning is employed for case 10 (1:3:1 aspect ratio). Bottom: The evolution of α when full cleaning is employed for case 11 (1:6:1 aspect ratio)

shearing box model in which the ideal MHD equations were solved. We chose to start by considering a cube with sides of equal length because we wished to have large integration times (1000 orbits) and a numerical dissipation that the same in all directions.

Our calculations shown that, without correction, there is a shift in the accretion rate (a shift in the turbulent transport rate). Such a shift is interesting due to the fact that there are shifts in spectra of accretion discs, which imply a

corresponding shift in accretion rate. However, in this case, the shift is unintentional and a by-product of the interpolation in the shearing box boundary conditions that introduce errors because of the interpolation that is a necessary part of the procedure. This error is unavoidable in such calculations and does remain small for low numbers of orbits. However, for large numbers of orbits the error is shown to compound to such an extent that the mean B_y field, which should be zero, grows and becomes larger in magnitude than the imposed B_z field. This error filters into the various components of both the velocity and magnetic fields.

In this paper we sought to consider the simple case of an imposed vertical magnetic field i.e. without a shift to a state where there was a mean field in more than one direction. As such we applied a simple fix to this issue that removes the error that is induced into the mean value of each of the components of the velocity and magnetic fields. This facilitated us to evaluate a long-term cumulative average for α , which is a better quantity when you wish to compare α values for different parameters. Following this procedure, we showed that increasing the resolution, for a fixed box size, gives rise to an increase in the value of α , which suggests that the values here are probably a lower bound for α values in these kind of simulations. This leads us to deduce that small scales are playing an important role in determining the rate of accretion. In an accretion disc the dissipative length-scale is much less than we considered here and so we conclude that in a disc there will be a significant enhancement to the rate of angular momentum transport.

As mentioned above, the work in the first part of this paper is not in the standard domain of the early work in a shearing box i.e. it was conducted in a cube with sides of equal length. This was selected to facilitate our desire for higher resolutions and extremely long integration times. However, it is of obvious interest to examine the effect of increasing the box length at modest resolutions. We found that increasing the box length led to a reduction in the mean value of α . This is attributed to the increased freedom for the parasitic instability as the box length is increased (see Goodman & Xu (1994) for a detailed discussion of this instability). We note here that while that increasing the resolution by a factor of four leads to a modest (15 box length is much more profound and increasing the box length by a factor of three leads to a reduction of α such that it is almost $2/3$ of its value for a box with length 1 in the y-direction.

While we acknowledge that there is still considerable working to be conducted in this area to fully understand the magnetorotational instability we believe that this paper is an important contribution to the field as it clearly demonstrates the need for great care in numerical calculations. Further it shows that, for the case of a imposed vertical magnetic field, α is non-negligible and it points to there existing sufficient transportation within a disc to give accretion in an appropriate time-scale.

The reader should note that what has been found here is for the case of a uniform vertical magnetic field and that this is very different to the case of a zero-mean magnetic field as considered by, for example, Pessah, Chan, Psaltis (2007) Fromang & Papaloizou (2008) and Fromang, Papaloizou, Lesur, Heinemann (2008), where α in many situations was found to be extremely small. Here we have shown that α increases as the scale of dissipa-

tion decreases and that it decreases as the length of the computational domain in the azimuthal direction is increased. It is not clear to what extent zero-mean flux calculations for long times are effected by the error that we found and we would suggest that all calculations in a shearing box check that mean quantities are maintained to expected values.

This paper does pose some questions of which the most obvious is whether or not a change in the balance of mean components of the magnetic field, along with the strength of the magnetic field, always gives rise to a change in the accretion rates. This issue is being investigated at present.

ACKNOWLEDGMENTS

We would like to thank Steve Balbus, John Hawley, Pierre Lesaffre and Jim Stone for suggestions and comments on during this work. We wish to thank the Ecole Normale Supérieure for the supercomputer known as JxB on which these calculations were carried out. We also wish to thank the referee for helpful suggestions.

REFERENCES

- Balbus, S. A. & Hawley, J. F. , 1991, *ApJ*, 376, 214.
 Balbus, S. A. & Hawley, J. F. , 1992, *ApJ*, 400, 610.
 Balbus, S. A. & Hawley, J. F. , 1998, *RvMP*, 70, 1, 1.
 Brandenburg, A, Nordlund, A., Stein, R. F., Torkelsson, U., 1995, *ApJ*, 446, 714.
 Fromang, S. A., Papaloizou, J. C. B., 2008, *A & A* accepted.
 Fromang, S. A., Papaloizou, J. C. B., Lesur, G., Heine-
 mann, T., 2008, *A & A* accepted.
 Goodman, J., Xu, Guohong , 1994, *ApJ*, 432, 213.
 Hawley, J. F., Gammie, C. F. & Balbus, S. A. , 1995, *ApJ*,
 440, 742.
 Hawley, J. F., Gammie, C. F. & Balbus, S. A. , 1996, *ApJ*,
 464, 690.
 Hawley, J. F., Stone, J. M., 1995, *Comput. Phys. Comm*,
 89, 127.
 Lesur, G. & Longaretti, P-Y. 2007, *MNRAS*, 378, 4, 1471.
 Pessah, M. E., Chan, C.K., Dimitrios, P., 2007, *ApJ*, 668,
 L51. e
 Stone, J. M., Norman, M. L. 1992, *APJS*, 80, 819.
 Shakura, N. I. & Sunyaev, R. A., 1973, *A & A*, 24, 337.
 Winters, W. F., Balbus, S. A. & Hawley, J. F., *MNRAS*,
 340, 519.